Theoretical Study of Spectroscopic Properties of Insulated Molecular Wires Formed by Substituted Oligothiophenes and Cross-Linked a-Cyclodextrin

ARTICLE *in* JOURNAL OF POLYMER SCIENCE PART B POLYMER PHYSICS · AUGUST 2011

Impact Factor: 3.83 · DOI: 10.1002/polb.22278

Theoretical Study of Spectroscopic Properties of Insulated Molecular Wires Formed by Substituted Oligothiophenes and Cross-Linked α-Cyclodextrin

Mateus F. Venâncio,[1] Clebio S. Nascimento, Jr.,[2] Cleber P. A. Anconi,[3] Juliana Fedoce Lopes,[1] Willian R. Rocha,[1] Hélio F. Dos Santos,[4] Wagner B. De Almeida[1]

[1]Laboratório de Química Computacional e Modelagem Molecular (LQC-MM), Departamento de Química, ICEx, Universidade Federal de Minas Gerais (UFMG), Campus Universitário, Pampulha, Belo Horizonte, MG 31270-901, Brazil

[2]Departamento de Ciências Naturais, Universidade Federal de São João Del Rei (UFSJ), Campus Dom Bosco, Praça Dom Helvécio, 74, São João Del Rei, MG 36301-160, Brazil

[3]Departamento de Química, Universidade Federal de Lavras (UFLA), Campus Universitário, Lavras, MG 37200-000, Brazil

[4]Núcleo de Estudos em Química Computacional (NEQC), Departamento de Química, ICE, Universidade Federal de Juiz de Fora (UFJF), Campus Universitário, Martelos, Juiz de Fora, MG 36036-330, Brazil

Correspondece to: W. B. De Almeida (E-mail: wagner@netuno.qui.ufmg.br)

Received 8 April 2011; revised 30 April 2011; accepted 2 May 2011; published online 18 May 2011
DOI: 10.1002/polb.22278

ABSTRACT: The inclusion compound formed between cross-linked α-cyclodextrin dimer and substituted oligothiophene, was investigated using density functional theory (DFT). Energy gap, spectroscopy (IR, UV–vis, ^{13}C NMR, and ^{1}H NMR) and first hyperpolarizability data were analyzed for the free species and inclusion compound, pp-PT@(αCD–αCD). The semiconducting property of the included pp-PT was not substantially affected on inclusion, with the energy gap increasing by only 10% after interaction with αCD–αCD. On the other hand, the nonlinear optical (NLO) response was significantly decreased, with the first hyperpolarizability, β, predicted to be just more than 60% lower for the [2]rotaxane than for free pp-PT, but still having considerable magnitude. This was explained by the two-state model based on the charge-transfer contribution to the electronic transitions. The sensitivity of electronic spectra might also be useful for the inclusion complex characterization. The IR spectrum was slightly sensitive to the host–guest interaction and the calculated ^{13}C NMR and ^{1}H NMR chemical shifts for the pp-PT guest showed appreciable variations of 5–10 and 1–1.5 ppm, respectively, and so can be used for the characterization of inclusion compounds. We concluded that the formation of inclusion complexes with CDs, seems indeed very promising and the use of encapsulating conducting material should be experimentally pursued. © 2011 Wiley Periodicals, Inc. J Polym Sci Part B: Polym Phys 49: 1101–1111, 2011

KEYWORDS: computer modeling; conjugated polymers; charge transfer; cyclodextrin; density functional theory (DFT)

INTRODUCTION Since the discovery of conducting characteristics of polyacetylene in 1977 by Shirakawa and coworkers,[1] a great scientific and technological effort has been devoting to the synthesis and applications of conjugated organic polymers.[2–4] In the field of organic conducting polymers, polythiophene (PT) and its derivatives continue to attract great interest for fundamental studies, synthesis, characterization, and potential applications as electronic devices.[5–12] PT derivatives with different substituents linked at the ends of the polymer chain might show distinct interchain interaction and π-conjugation in the polymer's backbone. On the basis of the molecular structure and property relationships, PT derivatives, such as those with electron-withdrawing (NO_2) and electron-donating (MeO) groups, that is, push–pull PT [pp-PT, Fig. 1(a)], should have different degrees of π-conjugation in the backbone of PT due to stereo and electronic effects. These groups and also the conjugation lengths can influence the molecular conformation increasing the gap energy.[7] Reviews on π-conjugated systems, including PT, have been published and provide comprehensive data concerning synthesis, characterization by several physical techniques, and applications.[13,14] Nevertheless, it is important to mention that a fundamental requirement for processing and application of any conjugated polymer as molecular electronic device is the solubility. In this sense, various oligothiophene with polymerization degree greater than six are insoluble in different solvents. Chemical changes on the polymer chain are, although a key strategy for improving the properties of this class of molecules. It is possible, however, that electrical properties will be strongly affected by the nature of the

Additional Supporting Information may be found in the online version of this article.

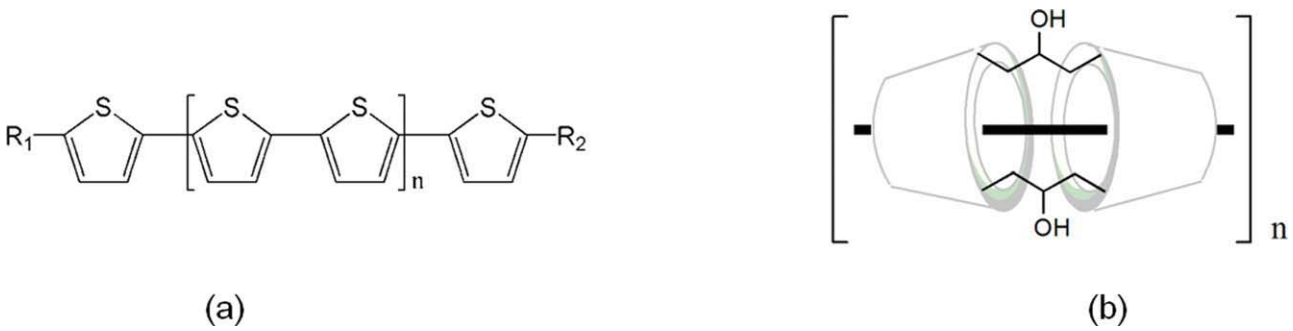

FIGURE 1 (a) General structure of substituted-PTs. For the methoxy-nitro-sexithiophene (pp-PT), $n = 2$, $R_1 = NO_2$ and $R_2 = OCH_3$. (b) General structure of a generic "molecular wire" formed by a semiconducting oligomer (black line) and the cross-linking CD.

substituent.[9] In this context, an alternative and viable strategy to improve the solubility of organic polymers is the formation of inclusion complexes with cyclodextrins (CDs), also called "molecular wires."

CD rotaxanes and CD polyrotaxanes whose structures consist of ring-shaped CDs with polymers or oligomers inserted into their cavities are important systems for host–guest chemistry.[15–17] In addition, they are also essential for the development of nanosized structures such as "molecular wires"[18–20] as a rigid molecular structure can be formed by coating with CD.[21] CDs are versatile hosts and their cavity size is regulated by the number of D-glucose units in each CD molecule (6, 7, and 8 for α-, β-, and γ-CD, respectively). A molecular tube can be created by a cross-linking of two adjacent α-CD units using a hydroxypropylene bridge[22] [Fig. 1(b)].

In the last years, our group has been applied theoretical quantum mechanical methods to study CD aggregates aiming to understand the structural arrangement and the stoichiometry of this class of compounds.[23–27] "Molecular wires" formation has been also reported in literature in both theoretical and experimental works.[28–35] In particular, when using CD rotaxanes for nanomolecular devices, knowing the electronic states is important to understand the operational mechanism as well as how to modulate electronic properties for further development of advanced materials with potential applications. Microscopic techniques such as atomic force microscopy and scanning tunneling microscopy have indicated an inclusion complex formation in which the polymer is fully covered by β-CD molecules[28] and also a molecular nanotube of cross-linked α-CD molecules.[31] Moreover, theoretical studies also showed that β-CD molecules can be used as an insulated near-planar configuration of polymers, with an optimized molecular structure and electronic configuration very similar to the one at the planar conformation.[29,32,36] In this field, most of theoretical research, however, has been limited to molecular structure study and has not targeted their electronic states and properties. Furthermore, the computational cost increases rapidly for large molecules, which makes difficult to study these supramolecular systems using any pure quantum mechanical high level of theory.[29,32,34,36] However, the continuous introduction of faster computers and new methodologies, which could enable the calculation of supramolecular electronic structures with remarkable precision, has provided us a new motivation to study a PT "molecular wire" by pure *ab initio* calculations, to obtain a more reliable structural and electronic analysis. In this context, the present study uses density functional theory (DFT)[37] to evaluate the molecular structure and electronic states of a PT derivative "molecular wire" and its respective CD rotaxane formed by a cross-linked dimeric α-CD structure [αCD–αCD; Fig. 1(b)]. In addition, the effect of the inclusion process on the molecular structure and electronic properties of substituted PT was also investigated.

COMPUTATIONAL DETAILS

Initially, the geometry of methoxy-nitro-sexithiophene, MeO-PT-NO_2, abbreviated here as pp-PT, a push–pull-substituted oligothiophene [Fig. 1(a)], was fully optimized without any geometrical or symmetry constraints at the DFT level using different LDA and GGA functionals, such as SVWN,[38–40] BLYP,[41,42] PBE1PBE,[42–44] and B3LYP.[41,45,46] It is important to mention that the sexithiophene structure was chosen because of its potential technological applications.[47] The basis set used in these calculations was the Pople's standard polarized split-valence 6-31G(d,p)[48–51] and a mixed basis set. This procedure, which was previously described by our group,[27] is very important because it enables DFT calculations of supramolecular systems, such as CDs, with a gain in terms of computational time without losing quality of structural and energetic properties. The key idea of this procedure is to treat the main atoms as those involved directly in the formation of hydrogen bonds, namely the oxygen, nitrogen, sulfur, and hydrogen atoms connected to them, with a set of basis functions containing more polarization and diffuse functions such as 6-31G(d,p) or 6-31++G(d,p), and the remaining atoms with a minimum basis STO-3G. CH_n groups, for example, are considered as expectators for the inclusion process, so are treated with the small basis set. This mixed basis set scheme is named hereafter as Gen1.

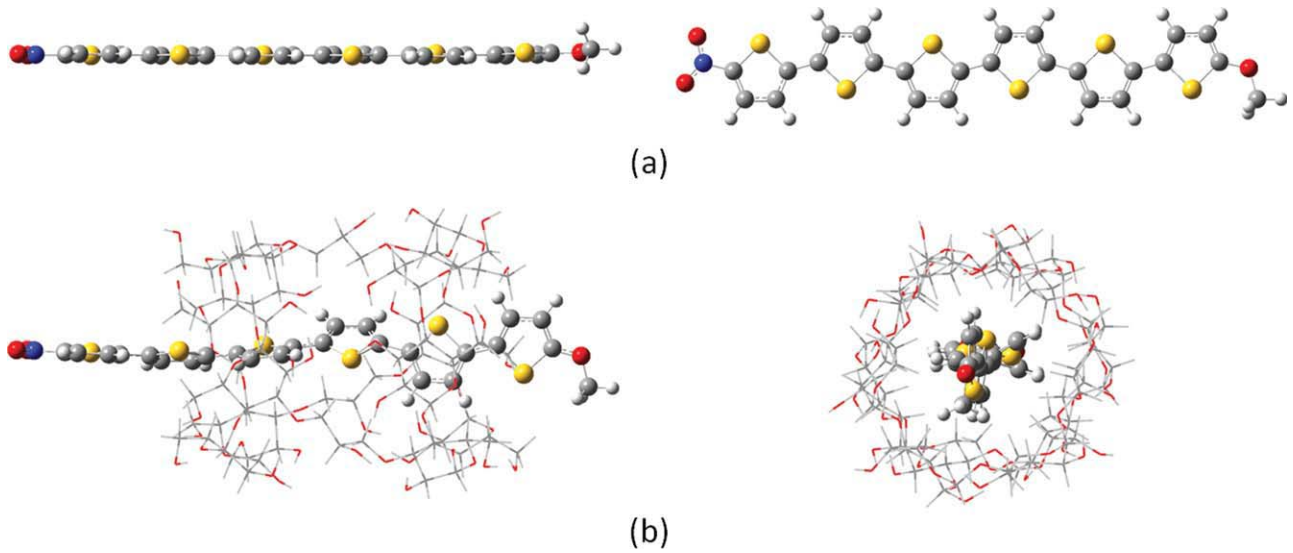

FIGURE 2 PBE1PBE/Gen1 fully optimized structures for the free pp-PT oligothiophene (a) and the inclusion complex (b).

Once the optimized geometry was obtained, we performed the calculation of the band gap through the highest occupied molecular orbital to the lowest unoccupied molecular orbital (HOMO/LUMO) energy difference that provides good estimation of the excitation energy.[52] It was found that the PBE1PBE functional yielded the best energy gap for pp-PT studied here compared with experiment (to be shown later), so this functional was used throughout this work. Furthermore, the geometry of cross-linked α-CD dimer, abbreviated as αCD–αCD [Fig. 1(b)], was fully optimized at the DFT using the PBE1PBE functional. As the host and inclusion complex treated here consist of a huge number of atoms, an alternative procedure to make pure *ab initio* calculations feasible is certainly welcome to perform DFT calculations with an adequate basis set. In this sense, to perform PBE1PBE calculations for all species including the complex pp-PT@(αCD–αCD), we adopted a procedure involving a mixed basis set function (Gen1). All the spectroscopic calculations were carried out with PBE1PBE/Gen1optimized geometries and using PBE1PBE/6-31G(d,p) single point calculations. This approach is usually symbolized as PBE1PB/6-31G(d,p)//PBE1PBE/Gen1. All calculations were carried using the Gaussian 03 quantum mechanical package.[53]

RESULTS AND DISCUSSION

Structural Analysis

Initially, a rapid structural analysis was carried out for the pp-PT species optimized at the DFT level using distinct functionals: SVWN, BLYP, PBE1PBE, and B3LYP with the basis set 6-31G(d,p). The average deviations for all the DFT results for bond lengths and torsion angles were 0.02 Å and 0.1°, respectively, when compared with experimentally obtained structural data.[54] This result demonstrated that pp-PT geometries predicted by LDA, GGA, and hybrid-GGA functional are almost identical. The geometry of the pp-PT@(αCD–αCD) inclusion complex was optimized with the PBE1PBE functional using the mixed basis set (Gen1), and also the 6-31G(d,p) basis set on all atoms. For the inclusion complex having 326 atoms, the Gen1 basis set contain 1928 basis functions, whereas the 6-31G(d,p) basis set have 3444 basis functions. Therefore, there is a considerable reduction in computational cost for the geometry optimization using the Gen1 basis set (∼45% less basis functions). The PBE1PBE/Gen1 fully optimized geometries for the free substituted oligothiophene and the inclusion complex are shown in Fig. 2. The optimized geometry of the inclusion complex at PBE1PBE/6-31G(d,p) level is almost identical to the structure optimized with the mixed basis set, PBE1PBE/Gen1 level. After inclusion, the pp-PT structure shows a torsion on the third to fourth dihedral angle between adjacent thiophene rings (S—C—C—S). For the pp-PT guest, the calculated dihedral angle was 27.0° at PBE1PBE/6-31G(d,p) and 31.5° at PBE1PBE/Gen1 level of theory. Therefore, besides the bond lengths, both the optimized structures, with the two different basis set used here, show practically the same distortion of the pp-PT guest molecule due to the complex formation, revealing that the PBE1PBE/Gen1 structure is indeed quite adequate for further calculations and studies. It can be seen from Fig. 2(b) that the guest molecule is partially included in the αCD–αCD with the nitro and methoxy groups outside the cavity and the pp-PT molecule is substantially distorted on complexation. The bond length alternation in the pp-PT backbone is represented in Fig. 3(a) and the inter-ring dihedral angles in Fig. 3(b). In this figure, the structural parameters (b and d) are measured from the NO_2 to OMe side, thus b1 and d1 are the bong length and torsion angle closest to NO_2 group. It is noticed that the difference between single and double bonds is less pronounced in the free oligothiophene, suggesting a more effective electron delocalization in the free species. The confinement of the guest molecule twists the pp-PT chain, mainly in the part of

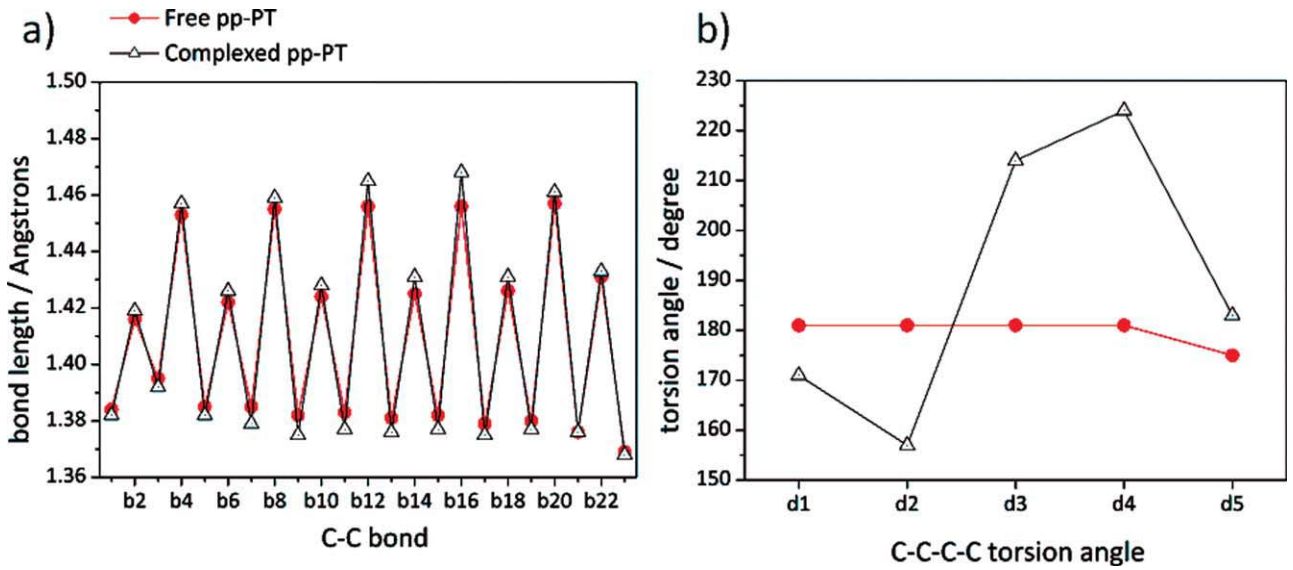

FIGURE 3 CC bond length (a) and dihedral angle (b) alternation for the pp-PT molecule free and complexed with d-α-CD. In this figure the structural parameters (b and d) are measured from the NO_2 to OMe side, thus, b1 and d1 are the bong length and torsion angle closest to NO_2 group.

the molecule included (d2–d4) as clearly shown in Fig. 2(b). The electrical properties of this class of compounds have been attributed to the backbone planarity and this torsion on inclusion could be viewed as an obstacle to use this complex as a potential molecular device. The theoretical spectroscopic analysis and optical properties calculations, however, show that torsion is not a major problem.

Spectroscopic Assignments

In addition to the calculation of geometrical parameters, spectroscopic theoretical data were obtained by electronic structure calculations. These results can assist the experimental characterization of this kind of inclusion compounds which is not so easily achieved. The variation of spectroscopic properties of the guest and host molecules on complexation is commonly used as an evidence or even confirmation of the inclusion complex formation. Therefore, the theoretical determination of spectroscopic quantities for free and complexed guest molecules is certainly a great help to experimentalists working on the field of supramolecular chemistry.[55–57] With this aim in mind, we carried out theoretical calculations of infra red (IR), ultra-violet and visible (UV–vis), and nuclear magnetic resonance (^{13}C NMR and ^{1}H NMR) spectra for the free species and the pp-PT@(αCD–αCD) inclusion complex using DFT level of theory.

The gauge-independent atomic orbital method[58] was applied for the calculation of the ^{13}C and ^{1}H magnetic shielding constants (σ) and the chemical shift (δ) for selected atoms obtained on the δ-scale relative to the tetramethylsilane (TMS) at the DFT level of theory, as previously described in the structural determination of anhydrotetracyline–platinum dichloride complex study reported by our group.[59] The ^{13}C NMR chemical shifts for the inclusion complex, showing the contributions of (αCD–αCD) dimer and pp-PT monomers, are shown in Fig. 4(a), with the carbon numbering scheme for the pp-PT given in Fig. 4(c). For this ^{13}C NMR spectra representation, the degeneracy parameter of 0.05 ppm was used to represent similar atoms. It can be seen from Fig. 4(a) that the 115–170 ppm region of the NMR spectra corresponds exclusively to the pp-PT carbons, after the inclusion. The only two carbon atoms that are at the same region dominated by the CD carbons are the C5 which is outside the cavity and shows $\delta = 104.6$ ppm and the methoxy carbon C4 with $\delta = 63.2$ ppm.

The analysis of the ^{13}C NMR spectra reveals that it is indeed possible to confirm the formation of an inclusion compound through a comparison between the ^{13}C NMR profiles for the free and included samples. To simplify the identification of chemical shift variation due to inclusion complex formation, ^{13}C NMR difference values (in ppm) between free and complexed (αCD–αCD) dimer and pp-PT monomers are shown in Fig. 4(b). The major changes observed for the pp-PT monomer are highlighted by the carbon assignments on the graph. A variation of the ^{13}C NMR in the range of 5–10 ppm in the PT carbon atoms is observed, which would be easily experimentally detected. The pp-PT carbons placed inside the αCD–αCD are more shifted specially to those localized near the bridge formation such as C11 with $\Delta\delta = 10.7$ ppm and C20, $\Delta\delta = 9.5$ ppm. The similarity of these two carbons is slightly broken by the different end-groups, but, they are quite related by the position on the thiophene ring as well as the chemical environment on inclusion. As expected, carbons that are not capped by the (αCD–αCD) dimer, C4, C5, and C12 on the methoxy side as well as C7, C17, and C22 on the nitro side do not show significant change for the chemical shielding. For the CD carbons, the larger differences are observed for the carbons on the covalent bridge. It is noteworthy that the ^{13}C NMR chemical shifts calculated with the complex geometry optimized with the

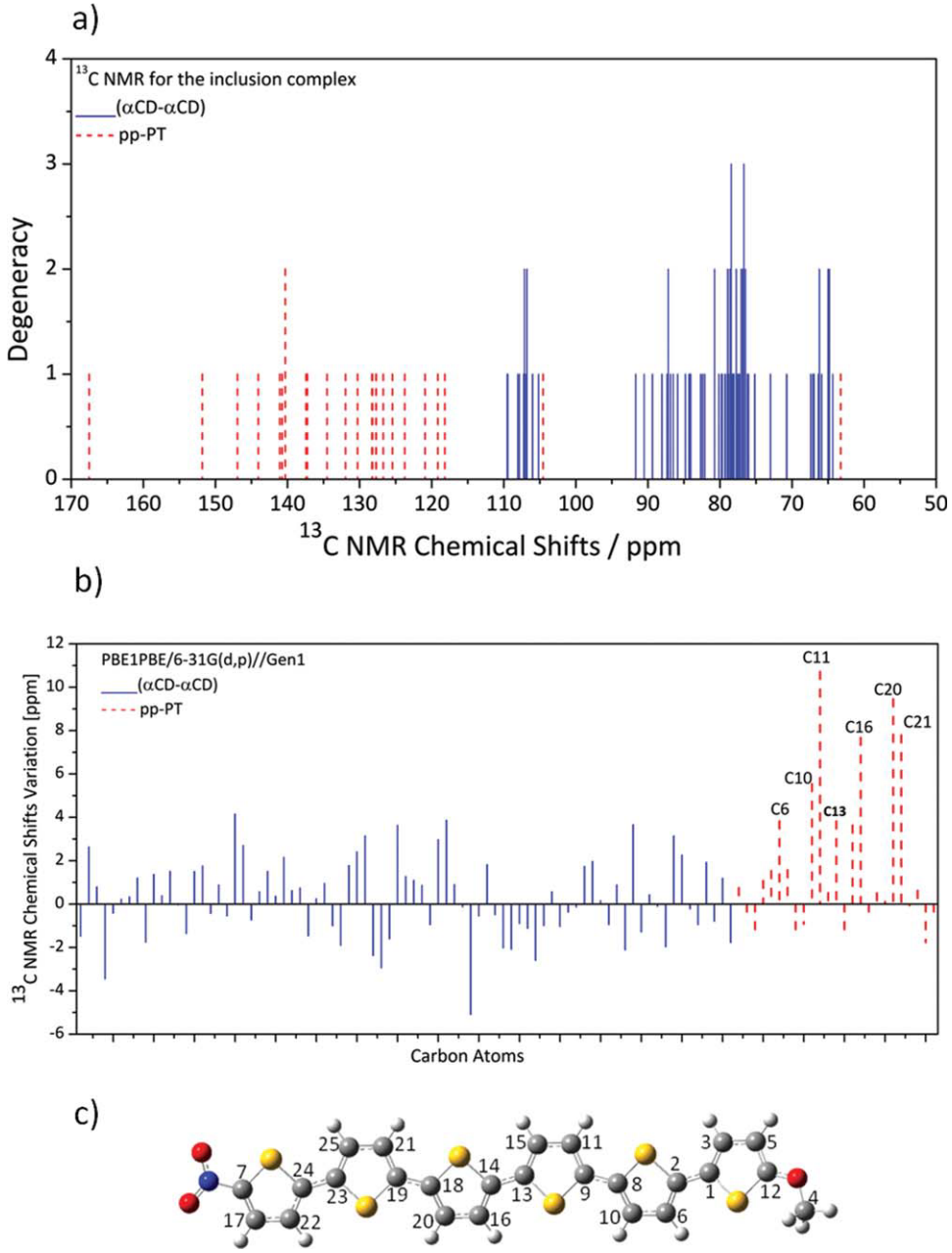

FIGURE 4 (a) The PBE1PBE/6-31G(d,p)//PBE1PBE/Gen1 ^{13}C NMR spectra for the inclusion complex. (b) PBE1PBE/6-31G(d,p)// PBE1PBE/Gen1^{13}C NMR chemical shift variation in ppm between calculated values for αCD–αCD and pp-PT free and its results on the inclusion complex and (c) carbon numbering scheme for the pp-PT species.

6-31G(d,p) basis set were almost identical to the values evaluated with the PBE1PBE/Gen1 optimized structure; this is a new evidence that this mixed basis set alternative can be used as an alternative strategy for calculations involving larger molecular systems.

The ^{1}H NMR chemical shifts [PBE1PBE/6-31G(d,p)// PBE1PBE/Gen1 values] for the pp-PT free monomer and the substituted PT subunit distorted on complexation are also shown in Supporting Information (see Supporting Information Fig. SI1). Once again, our analysis is focused on the chemical shift variation on inclusion, as represented in Fig. 5(a) for free pp-PT. Figure 5(b) shows the hydrogen labels used on the graph. From the data reported in Fig. 5(a), one can verify that all hydrogen nuclei are more deshielded in the inclusion complex, which is a consequence of the distortion in the guest structure and, mainly, due to the host–guest short contacts. This is even clearer when checking out the whole spectra shown in the Supporting Information. The signals for the protons of the pp-PT included in the dimer cavity split and the peaks are

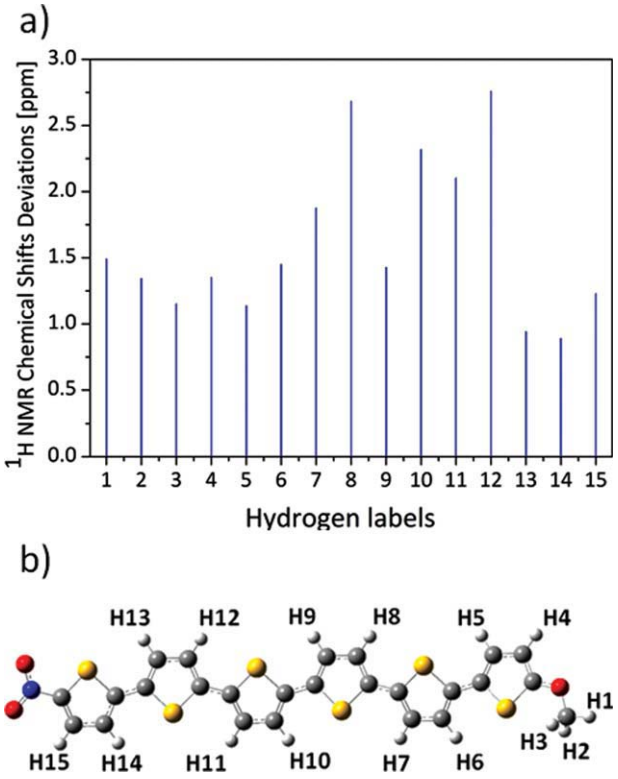

FIGURE 5 (a) PBE1PBE/6-31G(d,p)//PBE1PBE/Gen1 ^{1}HNMR chemical shift variation in ppm between calculated values for pp-PT free and its results on the inclusion complex. (b) The hydrogen numbering scheme.

downfield after inclusion takes place. It can be seen from a comparative analysis of Fig. 5(a) that the hydrogen atoms of pp-PT that are inside the CD cavity, as labeled in Fig. 5(b), exhibit a remarkable low field shift in the ^{1}H NMR as follows: H8 (2.68 ppm), H10 (2.32 ppm), H11 (2.10 ppm), and H12 (2.76 ppm). These variations would be easily detected in the NMR experiments. As expected, the hydrogen atoms not included in the cavity show a small change in the chemical shift values on complexation as its chemical environment does not change significantly. This result is very important, stressing the point that a theoretical and experimental analysis of ^{1}H NMR chemical shift changes for pp-PT can be of great aid for an unambiguous characterization of the structure of the inclusion compound, as hydrogens show a quite small spectral range, generally 15 ppm. The calculated (αCD–αCD) ^{1}H NMR spectra are quite complicated because of the many peaks that can be observed. These data are given as Supporting Information (see Supporting Information Fig. SI2) that also includes the variation on inclusion exclusively for hydrogens belonging to αCD–αCD structure. From these results, one can verify that the most affected hydrogens are those of the secondary hydroxyls on the intersection of the dimer formation. The signals corresponding to these hydrogens show a variation from 2.0 to 4.34 ppm.

The vibrational spectrum is the most computational demanding in the theoretical spectroscopic analysis. This is especially because of the need to access the second derivative of the energy with respect to the bond stretching and this procedure has to be carried out for all the bonds in the system. Therefore, for large systems as those studied here, it requires a very high computational effort to calculate all those data using a relatively large basis set which motivate the use of mixed basis set for these macromolecular systems. The IR spectrum for the pp-PT compound was calculated with 6-31G(d,p) and mixed (Gen1) basis sets. For the 3600–3000 cm^{-1} region, corresponding to C—H stretching modes, it was found that these vibrations were severely affected by the use of a small basis set (STO-3G) on the CH_n groups and must be ignored in the IR analysis using mixed basis sets, as already expected. The 2000–500 cm^{-1} region was very satisfactorily described by the mixed basis set, compared with the 6-31G(d,p) basis set results (free substituted PT) and it is the most important region to characterize the oligothiophene. Therefore, the IR spectra below the 2000 cm^{-1} region for the free and included substituted oligothiophene, using the mixed basis set can be analyzed safely to confirm the formation of the inclusion complex at a much lower computational cost as IR calculations with the 6-31G(d,p) basis set could not be performed because of the relative size of the molecular system and computational resources available. Figure 6 shows the IR spectra for free monomers and inclusion complex in the 2000–500 cm^{-1} region, as predicted by the PBE1PBE/Gen1 calculation. It can be promptly seen that the main bands of the free pp-PT are centered at 1633, 1549, and 1433 cm^{-1}. The two higher frequencies are due to CC stretching [ν(CC)], with the band at 1633 cm^{-1} assigned to the CC vibrations close to the donor group OMe and the absorption centered at 1549 cm^{-1} assigned to CC stretching of the molecular moiety close to the electron-withdrawing NO_2 group. This behavior was also observed for terthiophene structures with different push–pull groups.[60] The most intense band at 1433 cm^{-1} is mainly due to the stretching of the C_α—N and N—O bonds coupled with the CC stretching of the adjacent rings. The displacement vectors obtained for these vibrations are provided as Supporting Information (see Supporting Information Fig. SI3). These bands are slightly shifted toward higher frequency as a result of the confinement inside the αCD–αCD cavity and the consequent interference of the CD vibration modes. In the inclusion complex, these absorptions are found at 1640, 1557, and 1436 cm^{-1}, respectively, with decreasing relative intensity.

The electronic spectra were also calculated at the PBE1PBE/6-31G(d,p) level using the PBE1PBE/Gen1 geometries and the principal results for the pp-PT free, and after the inclusion process are plotted in Fig. 7 as band spectra simulated by fitting a sum of Gaussian functions.[61] All the detailed results including the calculated wavelength and the oscillator strength are given as Supporting Information (see Supporting Information Table SI1). It can be noted that the main absorption bands in Fig. 7 arise from two quite intense transitions, which are blue-shifted in the spectrum of the

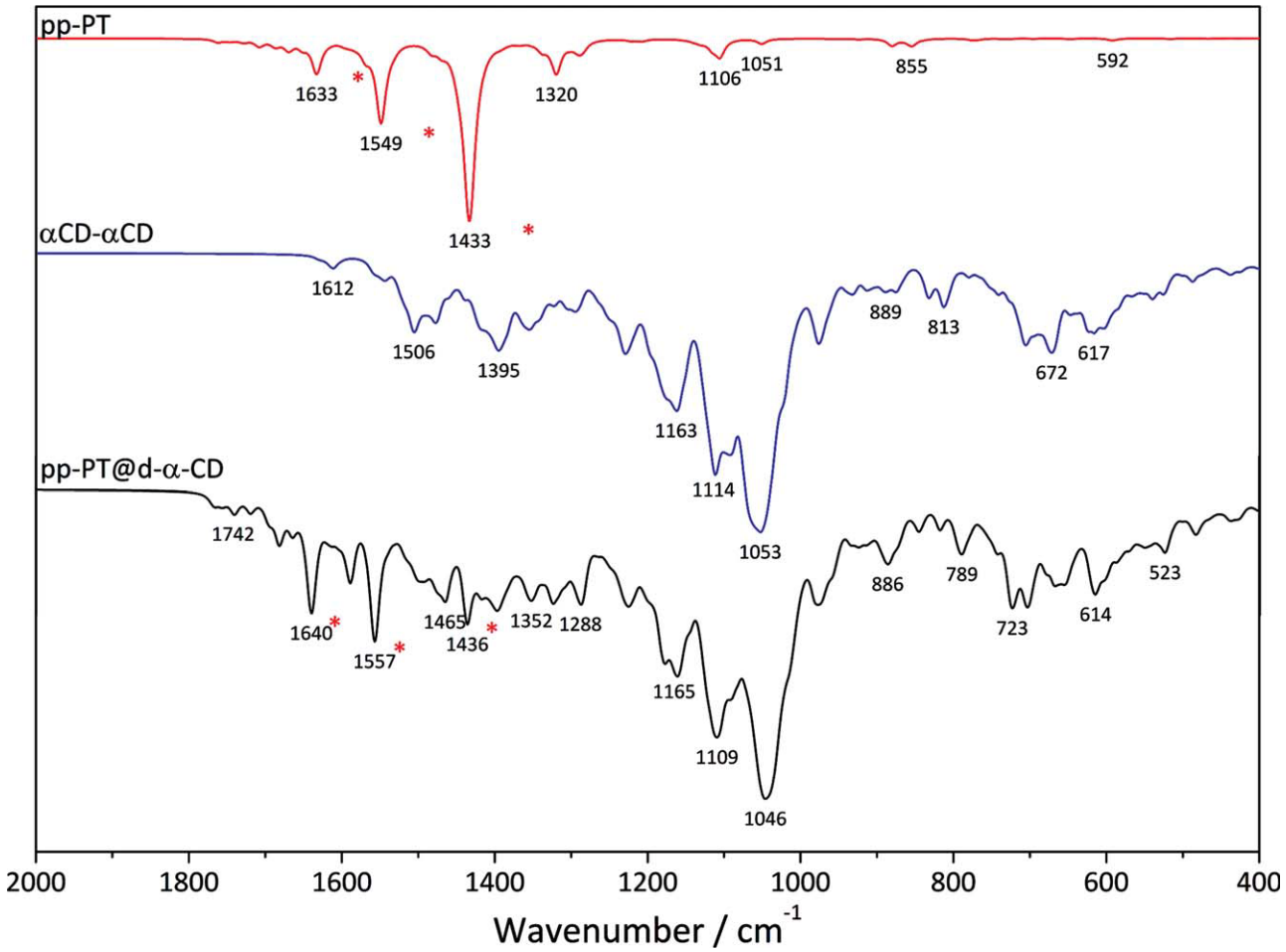

FIGURE 6 PBE1PBE/Gen1 IR spectra for free monomers and inclusion complex. The main bands assigned to the guest are indicated.

inclusion complex. The predicted overall shift was from 495 nm (free guest) to 459 nm (host–guest complex) that followed by a decrease in the intensity. The frontiers Kohn Sham MO are represented in Fig. 8. It can be seen from Fig. 8 that the HOMO is more localized on the thiophene rings close to the methoxy group, as expected for an electron-donor group. On the other hand, the LUMO is localized near to the nitro group. Therefore, the most intense transition (assigned to HOMO → LUMO) is attributed to a charge transfer. Experimental electronic spectra for oligothiophenes are scarce because of the low water solubility, however, for 6T-[3]rotaxane, which 6T represents a chemically modified sexithiophene, the absorption spectrum was obtained in aqueous solution[62] and showed a broad band centered at 449 nm, which is close to the value predicted here for pp-PT-[2]rotaxane, $\lambda_{max} = 459$ nm. This band is, however, attributed to a π–π^* transition which is expected for a nonmodified PT because HOMO and LUMO are π-type orbitals delocalized over all the backbone structure. Another experimental example from the literature is a nonlinear PT, synthesized as a self-insulated structure, which the thiophene backbone is planar improving the effective conjugation length and consequently the charge mobility.[63] The structure designed here, NO_2-6T-OMe thus behaves as a push–pull system with the HOMO–LUMO transition accounts for an intense absorption corresponding to a charge-transfer absorption band. This charge-transfer band was reported before[60,64] to explain the electronic spectra of push–pull PTs with a donor group on one side end and an electron-withdrawing group on the other side. This charge transfer from the electron-donor side to the electron-acceptor side of the molecule is one of the requirements to present attractive nonlinear optical (NLO) properties which will be evaluated at the next section.[65]

Electric and Optical Properties

The energy gap values were calculated at distinct DFT levels and basis sets. All these results are provided as Supporting Information (see Supporting Information Table SI2). It can be seen that the agreement for the free substituted oligothiophene with the experimental data is quite good when the PBE1PBE functional is used, which is the reason to choose this functional in the work reported here. It can be seen that the energy gap (2.46 eV) for the free pp-PT calculated at the PBE1PBE/6-31G(d,p)//PBE1PBE/Gen1 level is in exceptional

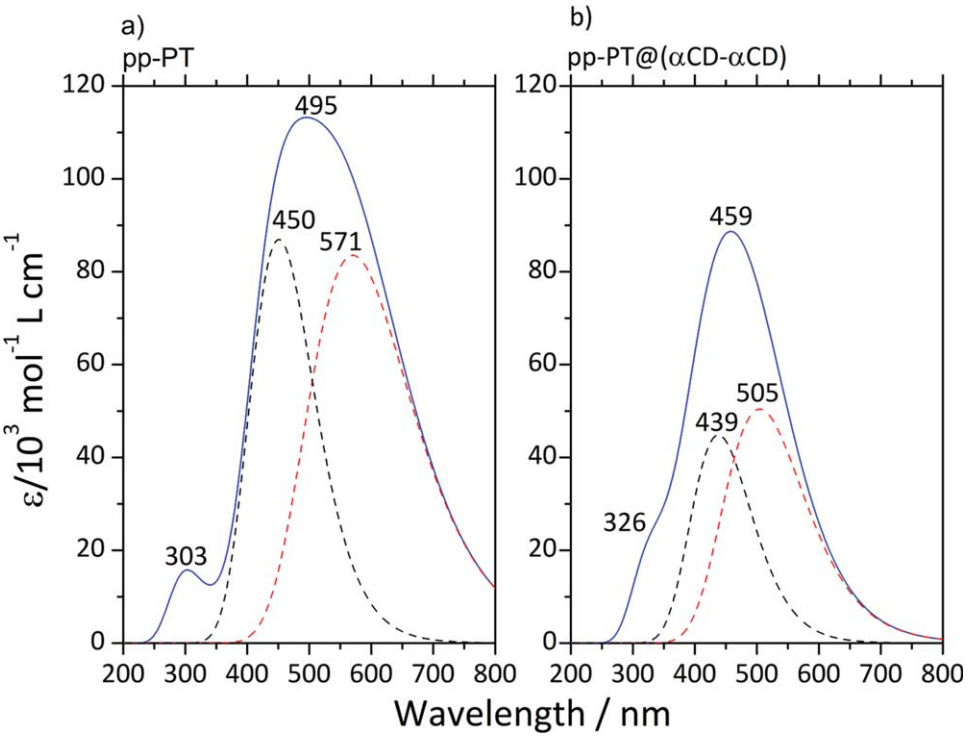

FIGURE 7 PBE1PBE/6-31G(d,p)//PBE1PBE/Gen1 electronic spectra for free monomers and inclusion complex.

agreement with experiment value,[66] 2.47 eV. It is known that control of the band gap (E_g) of organic materials is fundamental for building devices and furthermore reducing its value is desired to enhance the intrinsic charge carrier's population. Although there is some controversy surrounding the interpretation of DFT orbital energies, the HOMO/LUMO energy difference offers a very good estimate of band gaps. It should be noted that the HOMO/LUMO gap at the *ab initio* level does not closely relate to excitation energies due to the absence of orbital relaxation effects.[15]

An important result is the energy gap value for the pp-PT@αCD–αCD inclusion complex. It shows that the inclusion of oligothiophene in the hollow cross-linked αCD–αCD tube causes a slight increase on the energy gap from 2.49 to 2.78 eV [∼10% larger at the PBE1PBE/6-31G(d,p) level]. This increase can qualitatively be attributed to the reduction in the planarity of the polymer, as the increase of energy gap can be interpreted as a factor that hinders the conduction of electricity by the polymer. Moreover, the relative position of the orbitals participating in the conductance directly influences the ability of a material to be classified as a conductor, as the property is best seen in the case studied when the polymer is completely planar. This can be illustrated, for example, by a π-conjugated polymer covalently capped by a permethylated α-CDs, which keeps the linearity of the backbone structure on the inclusion and subsequent polymerazation[67] providing a highly semiconductor wire. From the energy gap predicted for the inclusion complex, it can be seen that the encapsulated substituted oligothiophene does not lose the semiconducting properties and, therefore, the use of inclusion compounds in the material science area can be viewed as a very promising experimental procedure. From our theoretical results, it can be inferred that the use of conducting materials in the form of inclusion compounds seems quite viable. The intermolecular interactions responsible for the formation of the inclusion complex do not cause great disturbance on the frontier molecular orbitals of the oligothiophene and so, has no great effect on the calculated energy gap as can be seen in Fig. 8.

Another important issue is the effect of the inclusion complex formation on the NLO response. This is also of great relevance as new material exhibiting NLO properties of acceptable magnitude may be conceived as inclusion compounds. Table 1 shows the electric properties calculated for the systems studied in this article, namely pp-PT, αCD–αCD, and pp-PT@αCD–αCD. It is interesting to note the change in the first hyperpolarizability, β, which decreases significantly (60%) on inclusion into the αCD–αCD cavity, although its value is still considerably large (>100 e.s.u.). This result can be partially understood on the basis of the two-state model proposed by Oudar and Chemla[68,69] to explain the high value of β for such push–pull organic chromophores. According to this model, the total β can be represented by the sum of two contributions (eq 1), accounting for the conjugated π-network (β_{add}) and charge transfer (β_{CT}).

$$\beta = \beta_{add} + \beta_{CT} \quad (1)$$

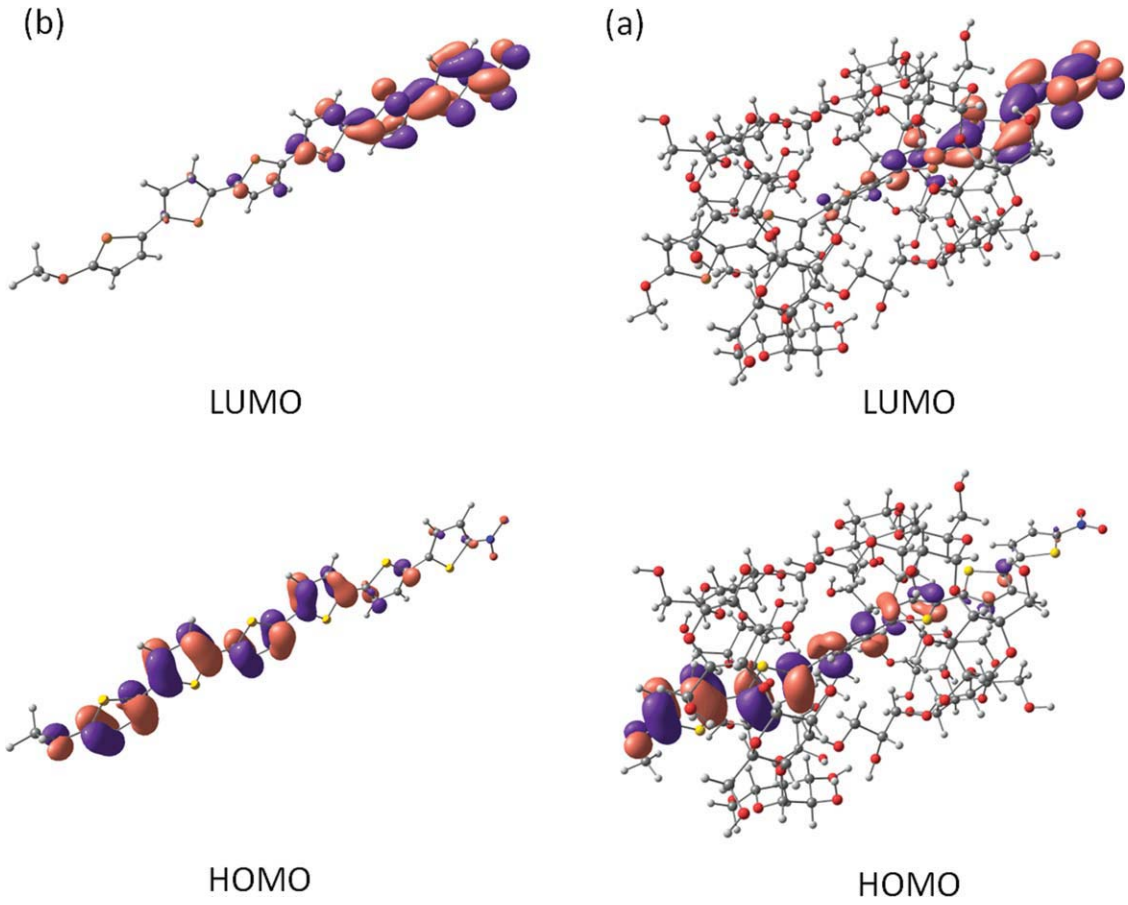

FIGURE 8 PBE1PBE/6-31G(d,p)//PBE1PBE/Gen1 frontier KS orbitals for (a) free pp-PT and (b) inclusion complex. Isovalue = 0.02.

The charge-transfer contribution is described by the interaction of two levels, namely ground state (g) and first excited state (e), following the general relationship given by eq 2.

$$\beta_{CT} \propto \frac{f_{ge}\Delta\mu_{ge}}{\Delta E_{ge}^3} \quad (2)$$

where $\Delta\mu_{ge}$ is the change in the dipole moment and f_{ge} and ΔE_{ge} are the oscillator strength and energy of CT transition, respectively. To apply the previous relations, the electronic spectra data given in UV–vis calculations (Supporting Information Table SI1) and Fig. 7 were used. As previously discussed, the data clearly show a blue-shift in the lowest energy transitions in addition to a decrease in their intensities on inclusion. It can also be noted that the main absorption bands in Fig. 7 arise from two quite intense transitions. Thus, using a rough assumption of constant $\Delta\mu_{ge}$ before and after inclusion, the values for f_{ge} (sum of the oscillator strength of two most intense transitions) and ΔE_{ge} from Fig. 7, the ratio β_{CT}(pp-PT)/β_{CT}(pp-PT@αCD–αCD) could be calculated. The result was 2.24, which agrees quite well to the actual value of 2.76 calculated using the values from Table 1. Thus, we can conclude that the charge transference interaction should play a primary role on the NLO properties of such molecule, as the CT process slightly less favorable in the inclusion compound.

CONCLUSIONS

In this study, the inclusion complex between cross-linked α-CD dimer (αCD–αCD) and substituted oligothiophene was investigated aiming to evaluate the encapsulation effect on the structural, electric, and spectroscopic properties of the guest oligothiophene molecule. The PBE1PBE functional was used with the 6-31G(d,p) basis set, which yielded the energy gap value of 2.49 eV, in very good agreement with the experimental value of 2.47 eV for the free oligothiophene. To save computer time, a mixed basis set was also used, where the minimal STO-3G basis set was used for C and H atoms

TABLE 1 Electric Properties: Dipole Moment (μ), Average Polarizability ($\langle\alpha\rangle$) and First Hyperpolarizability ($\langle\beta\rangle$) Calculated for (αCD–αCD), Push–Pull Oligothiophene (pp-PT) and pp-PT@(αCD–αCD) Inclusion Complex

	μ ($\times 10^{-18}$ e.s.u.)	$\langle\alpha\rangle$ ($\times 10^{-23}$ e.s.u.)	$\langle\beta\rangle$ ($\times 10^{-30}$ e.s.u.)
αCD–αCD	4.0	15.2	1.4
pp-PT	9.8	9.5	738.4
pp-PT@ (αCD–αCD)	10.2	23.0	267.4

Values obtained at PBE1PBE/6-31G(d,p)//Gen1 level.

belonging to CH_n groups considered as spectators, for geometry optimization of the complex, showing to be very adequate for structure and energy gap calculations likewise. We found that the energy gap of the oligothiophene guest molecule is not substantially affected by the formation of the inclusion complex, for which the predicted value was 2.78 eV, ~10% larger than the energy gap for the free pp-PT. Therefore, the use of encapsulating conducting material seems very promising. The calculation of the first hyperpolarizability revealed that the β value of the NLO response is considerably attenuated because of the inclusion complex formation but does not exclude the use of new materials as inclusion compounds, still having an appreciable magnitude. The decrease of β (~60%) was successfully explained by the two-state model, concluding that most of the NLO response comes from a charge-transfer process.

For the characterization of the inclusion compound, the DFT calculation of ^{13}C NMR and ^{1}H NMR chemical shifts, IR and UV–vis spectra appears to be a quite useful strategy. The spectroscopic evidence of the inclusion complex formation can be summarized as follows: (i) the most intense absorption in the visible region is blue-shifted from 495 to 459 nm; (ii) the three main IR bands at 1633, 1549, and 1433 cm^{-1} are found at higher frequencies in the rotaxane, at 1640, 1557, and 1436 cm^{-1}; (iii) the PBE1PBE/6-31G(d,p) ^{13}C NMR and ^{1}H NMR chemical shifts calculated for the substituted PT showed a variation of 5–10 and 1–1.5 ppm, respectively, due to the formation of the inclusion compound, what can be easily observed in the experimental NMR spectra; therefore, it can be of real practical use in combination with other spectroscopic data for the validation of inclusion complex structure.

One can design a larger structure from the complex studied here, using a greater PT or connecting several CDs unities by adding more cross-linked α-CD dimmers, which can mimic more faithfully a supramolecular system. Our results strongly motivate the use of theoretical (DFT) and experimental spectroscopic quantities for the characterization of inclusion compounds, which is not an easy experimental task and, therefore, a combined experimental/theoretical approach seems very promising. In addition, as PT and its derivatives are still of great experimental interest but have well-known inconvenience to be used as molecular electronic device due to the insolubility in various solvents, we found that their use in the form of encapsulating conducting material, which is an interesting alternative to improve the solubility of organic polymers, can be very successful and should be considered in further experimental investigations.

ACKNOWLEDGMENTS

The authors would like to thank the Brazilian Agencies CNPq, CAPES, and FAPEMIG for the support to our laboratories. This work is a collaboration research project of members of the Rede Mineira de Química (RQ-MG) supported by FAPEMIG. W. R. Rocha also would like to thank the INCT-CATÁLISE for financial support.

REFERENCES AND NOTES

1 Chiang, C. K.; Fincher, C. R.; Park, Y. W.; Heeger, A. J.; Shirakawa, H.; Louis, E. J.; Gau, S. C.; MacDiarmid, A. G. *Phys. Rev. Lett.* **1977,** *39*, 1098–1101.

2 Pokhodenko, V. D.; Krylov, V. A. *Theor. Exp. Chem.* **1994,** *30*, 91–105.

3 Günes, S.; Neugebauer, H.; Sariciftci, N. S. *Chem. Rev.* **2007,** *107*, 1324–1338.

4 Skotheim, T. A.; Reynolds, J. R. Conjugated Polymers: Theory, Synthesis, Properties, and Characterization; Taylor and Francis Group: USA, **2007.**

5 Kitamura, C.; Tanaka, S.; Yamashita, Y. *Chem. Mater.* **1996,** *8*, 570–578.

6 De Oliveira, M. A.; Dos Santos, H. F.; De Almeida, W. B. *Phys. Chem. Chem. Phys.* **2000,** *2*, 3373–3380.

7 De Oliveira, M. A.; Duarte, H. A.; Pernaut, J. M.; De Almeida, W. B. *J. Phys. Chem. A* **2000,** *104*, 8256–8262.

8 Heeger, A. J. *J. Phys. Chem. B* **2001,** *105*, 8475–8491.

9 De Oliveira, M. A.; De Almeida, W. B.; Dos Santos, H. F. *J. Braz. Chem. Soc.* **2004,** *15*, 832–838.

10 Bundgaard, E.; Krebs, F. C. *Polym. Bull.* **2005,** *55*, 157–164.

11 Hou, J. H.; Yang, C. H.; Qiao, J.; Li, Y. F. *Synth. Met.* **2005,** *150*, 297–304.

12 Bundgaard, E.; Krebs, F. C. *Macromolecules* **2006,** *39*, 2823–2831.

13 Becker, R. S.; Demelo, J. S.; Macanita, A. L.; Elisei, F. *Pure Appl. Chem.* **1995,** *67*, 9–16.

14 Roncali, J. *Chem. Rev.* **1997,** *97*, 173–275.

15 Nepogodiev, S. A.; Stoddart, J. F. *Chem. Rev.* **1998,** *98*, 1959–1976.

16 Takahashi, K. *Chem. Rev.* **1998,** *98*, 2013–2034.

17 Engeldinger, E.; Armspach, D.; Matt, D. *Chem. Rev.* **2003,** *103*, 4147–4173.

18 Taylor, P. N.; O'Connell, M. J.; McNeill, L. A.; Hall, M. J.; Aplin, R. T.; Anderson, H. L. *Angew. Chem., Int. Ed.* **2000,** *39*, 3456–3460.

19 Stanier, C. A.; Alderman, S. J.; Claridge, T. D. W.; Anderson, H. L. *Angew. Chem., Int. Ed.* **2002,** *41*, 1769–1772.

20 Michels, J. J.; O'Connell, M. J.; Taylor, P. N.; Wilson, J. S.; Cacialli, F.; Anderson, H. L. *Chem. Eur. J.* **2003,** *9*, 6167–6176.

21 Wenz, G.; Han, B. H.; Muller, A. *Chem. Rev.* **2006,** *106*, 782–817.

22 Harada, A.; Li, J.; Kamachi, M. *Nature* **1993,** *364*, 516–518.

23 Anconi, C. P. A.; Nascimento, C. S.; De Almeida, W. B.; Dos Santos, H. F. *J. Incl. Phenom. Macrocycl. Chem.* **2008,** *60*, 25–33.

24 Anconi, C. P. A.; Nascimento, C. S.; De Almeida, W. B.; Dos Santos, H. F. *J. Braz. Chem. Soc.* **2008,** *19*, 1033–1040.

25 Anconi, C. P. A.; Nascimento, C. S.; De Almeida, W. B.; Dos Santos, H. F. *J. Phys. Chem. B* **2009,** *113*, 9762–9769.

26 Nascimento, C. S.; Anconi, C. P. A.; Dos Santos, H. F.; De Almeida, W. B. *J. Phys. Chem. A* **2005,** *109*, 3209–3219.

27 Nascimento, C. S.; Anconi, C. P. A.; Lopes, J. F.; Dos Santos, H. F.; De Almeida, W. B. *J. Incl. Phenom. Macrocycl. Chem.* **2007,** *59*, 265–277.

28 Yoshida, K.; Shimomura, T.; Ito, K.; Hayakawa, R. *Langmuir* **1999,** *15*, 910–913.

29 Belosludov, R. V.; Mizuseki, H.; Ichinoseki, K.; Kawazoe, Y. *Jpn. J. Appl. Phys. Part 1: Regul. Pap. Short Notes Rev. Pap.* **2002,** *41*, 2739–2741.

30 Cacialli, F.; Wilson, J. S.; Michels, J. J.; Daniel, C.; Silva, C.; Friend, R. H.; Severin, N.; Samori, P.; Rabe, J. P.; O'Connell, M. J.; Taylor, P. N.; Anderson, H. L. *Nat. Mater.* **2002,** *1*, 160–164.

31 Shimomura, T.; Akai, T.; Abe, T.; Ito, K. *J. Chem. Phys.* **2002,** *116*, 1753–1756.

32 Belosludov, R. V.; Sato, H.; Farajian, A. A.; Mizuseki, H.; Kawazoe, Y. *Thin Solid Films* **2003,** *438*, 80–84.

33 Shimomura, T.; Akai, T.; Fujimori, M.; Heike, S.; Hashizume, T.; Ito, K. *Synth. Met.* **2005,** *153*, 497–500.

34 Belosludov, R. V.; Farajian, A. A.; Kikuchi, Y.; Mizuseki, H.; Kawazoe, Y. *Comput. Mater. Sci.* **2006,** *36*, 130–134.

35 Taniguchi, M.; Kawai, T. *Chem. Phys. Lett.* **2006,** *431*, 127–131.

36 Belosludov, R. V.; Sato, H.; Farajian, A. A.; Mizuseki, H.; Ichinoseki, K.; Kawazoe, Y. *Jpn. J. Appl. Phys. Part 1: Regul. Pap. Short Notes Rev. Pap.* **2003,** *42*, 2492–2494.

37 Parr, R. G.; Yang, W. Density-Functional Theory of Atoms and Molecules; Oxford University Press: Oxford, **1989.**

38 Hohenberg, P.; Kohn, W. *Phys. Rev. B* **1964,** *136*, B864–B871.

39 Kohn, W.; Sham, L. J. *Phys. Rev.* **1965,** *140*, 1133–1138.

40 Slater, C. The Self-Consistent Field for Molecular and Solids, Quantum Theory of Molecular and Solids; McGraw-Hill: New York, **1974;** Vol. *4*.

41 Becke, A. D. *Phys. Rev. A* **1988,** *38*, 3098–3100.

42 Perdew, J. P. *Phys. Rev. B* **1986,** *33*, 8822–8824.

43 Perdew, J. P.; Burke, K.; Ernzerhof, M. *Phys. Rev. Lett.* **1996,** *77*, 3865–3868.

44 Perdew, J. P.; Burke, K.; Wang, Y. *Phys. Rev. B* **1996,** *54*, 16533–16539.

45 Becke, A. D. *J. Chem. Phys.* **1993,** *98*, 5648–5652.

46 Lee, C.; Yang, W.; Parr, R. G. *Phys. Rev. B* **1988,** *37*, 785–789.

47 Barbarella, G.; Zambianchi, M.; Antolini, L.; Ostoja, P.; Maccagnani, P.; Bongini, A.; Marseglia, E. A.; Tedesco, E.; Gigli, G.; Cingolani, R. *J. Am. Chem. Soc.* **1999,** *121*, 8920–8926.

48 Ditchfield, R.; Hehre, W. J.; Pople, J. A. *J. Chem. Phys.* **1971,** *54*, 724–728.

49 Hehre, W. J.; Ditchfield, R.; Pople, J. A. *J. Chem. Phys.* **1972,** *56*, 2257–2261.

50 Hariharan, P. C.; Pople, J. A. *Theor. Chim. Acta* **1973,** *28*, 213–222.

51 Hariharan, P. C.; Pople, J. A. *Mol. Phys.* **1974,** *27*, 209–214.

52 Alguno, A. C.; Chung, W. C.; Bantaculo, R. V.; Vequizo, R. M.; Miyata, H.; Ignacio, A. M.; Bacala, A. M. *Tech. J.* **1999,** *2*, 215–219.

53 Frisch, M. J.; Trucks, G. W.; Schlegel, H. B.; Scuseria, G. E.; Robb, M. A.; Cheeseman, J. R.; Montgomery, J. A., Jr.; Vreven, T.; Kudin, K. N.; Burant, J. C.; Millam, J. M.; Iyengar, S. S.; Tomasi, J.; Barone, V.; Mennucci, M.; Cossi, M.; Scalmani, G.; Rega, N.; Petersson, G. A.; Nakatsuji, H.; Hada, M.; Ehara, M.; Toyota, K.; Fukuda, R.; Hasegawa, J.; Ishida, M.; Nakajima, T.; Honda, Y.; Kitao, O.; Nakai, H.; Klene, M.; Li, X.; Knox, J. E.; Hratchian, H. P.; Cross, J. B.; Bakken, V.; Adamo, C.; Jaramillo, J.; Gomperts, R.; Stratmann, R. E.; Yazyev, O.; Austin, A. J.; Cammi, R.; Pomelli, C.; Ochterski, J. W.; Ayala, P. Y.; Morokuma, K.; Voth, G. A.; Salvador, P.; Dannenberg, J. J.; Zakrzewski, V. G.; Dapprich, S.; Daniels, A. D.; Strain, M. C.; Farkas, O.; Malick, D. K.; Rabuck, A. D.; Raghavachari, K.; Foresman, J. B.; Ortiz, J. V.; Cui, Q.; Baboul, A. G.; Clifford, S.; Cioslowski, J.; Stefanov, B. B.; Liu, G.; Liashenko, A.; Piskorz, P.; Komaromi, I.; Martin, R. L.; Fox, D. J.; Keith, T.; Al-Laham, M. A.; Peng, C. Y.; Nanayakkara, A.; Challacombe, M.; Gill, P. M. W.; Johnson, B.; Chen, W.; Wong, M. W.; Gonzalez, C.; Pople, J. A. Gaussian 03, Revision D.01. Gaussian, Inc.: Wallingford, CT, **2004.**

54 Horowitz, G.; Bachet, B.; Yassar, A.; Lang, P.; Demanze, F.; Fave, J. L.; Garnier, F. *Chem. Mater.* **1995,** *7*, 1337–1341.

55 De Sousa, F. B.; Denadai, A. M. L.; Lula, I. S.; Lopes, J. F.; Dos Santos, H. F.; De Almeida, W. B.; Sinisterra, R. D. *Int. J. Pharm.* **2008,** *353*, 160–169.

56 De Sousa, F. B.; Denadai, A. M. L.; Lula, I. S.; Nascimento, C. S.; Fernandes, N. S. G.; Lima, A. C.; De Almeida, W. B.; Sinisterra, R. D. *J. Am. Chem. Soc.* **2008,** *130*, 8426–8436.

57 Dos Santos, H. F.; Duarte, H. A.; Sinisterra, R. D.; Mattos, S. V. D.; De Oliveira, L. F. C.; De Almeida, W. B. *Chem. Phys. Lett.* **2000,** *319*, 569–575.

58 Wolinski, K.; Hinton, J. F.; Pulay, P. *J. Am. Chem. Soc.* **1990,** *112*, 8251–8260.

59 Dos Santos, H. F.; Marcial, B. L.; De Miranda, C. F.; Costa, L. A. S.; De Almeida, W. B. *J. Inorg. Biochem.* **2006,** *100*, 1594–1605.

60 Casado, J.; Pappenfus, T. M.; Miller, L. L.; Mann, K. R.; Orti, E.; Viruela, P. M.; Pou-Amerigo, R.; Hernandez, V.; Navarrete, J. T. L. *J. Am. Chem. Soc.* **2003,** *125*, 2524–2534.

61 Dos Santos, H. F.; De Almeida, W. B.; Zerner, M. C. *J. Chem. Soc., Perkin Trans. 2* **1998,** *11*, 2519–2525.

62 Sakamoto, K.; Takashima, Y.; Yamaguchi, H.; Harada, A. *J. Org. Chem.* **2007,** *72*, 459–465.

63 Sugiyasu, K.; Honsho, Y.; Harrison, R. M.; Sato, A.; Yasuda, T.; Seki, S.; Takeuchi, M. *J. Am. Chem. Soc.* **2010,** *132*, 14754–14756.

64 Higuchi, H.; Uraki, Y.; Yokota, H.; Koyama, H.; Ojima, J.; Wada, T.; Sasabe, H. *Bull. Chem. Soc. Jpn.* **1998,** *71*, 483–495.

65 Paschoal, D.; Costa, M. F.; Junqueira, G. M. A.; Dos Santos, H. F. *J. Comput. Methods Sci. Eng.* **2010,** *10*, 239–256.

66 Garcia, P.; Pernaut, J. M.; Hapiot, P.; Wintgens, V.; Valat, P.; Garnier, F.; Delabouglise, D. *J. Phys. Chem.* **1993,** *97*, 513–516.

67 Terao, J.; Tanaka, Y.; Tsuda, S.; Kambe, N.; Taniguchi, M.; Kawai, T.; Saeki, A.; Seki, S. *J. Am. Chem. Soc.* **2009,** *131*, 18046–18047.

68 Oudar, J. L.; Chemla, D. S.; Batifol, E. *J. Chem. Phys.* **1977,** *67*, 1626–1635.

69 Oudar, J. L.; Chemla, D. S. *J. Chem. Phys.* **1977,** *66*, 2664–2668.